Metallized $Ni(OH)_2 \cdot NiO/FeOOH$ on Ni foam as Highly Effective Water Oxidation Catalyst Prepared by Surface Treatment: Oxidation-Corrosion Equilibrium

Fei Wang,† Xiaoxian Sun,† Yi Wang,† Huawei Zhou,†,* Jie Yin,†,* Xianxi Zhang†

† School of Chemistry and Chemical Engineering; College of Materials Science and Engineering; Shandong Provincial Key Laboratory/Collaborative Innovation Center of Chemical Energy Storage; Liaocheng University; Liaocheng 252059, China.

ABSTRACT: The surface treatment method has a great influence on the structure and properties of applied materials for interface catalysis. In this study, we prepare $Ni(OH)_2 \cdot NiO/FeOOH$ by surface treatment in acid solution using oxidation-corrosion equilibrium (OCE). For comparison, we also treat Ni foam with the same process in alkaline solution. $Ni(OH)_2 \cdot NiO/FeOOH$ can arrive steady-morphology and metallization by oxidation-corrosion equilibrium and exhibits superior catalytic activity as water oxidation catalyst. $Ni(OH)_2 \cdot NiO/FeOOH$(OCE) needs only 232 mV to reach a current density of 10 mA cm^{-2}, while it is 254 mV for a reference IrO_2/Ni foam. The mechanism study shows that the small charge transfer resistance (2.04 Ωcm^2) is favorable for the rapid interface electron exchange between $Ni(OH)_2 \cdot NiO/FeOOH$(OCE) and reactive species in water oxidation. In addition, the results of X-ray photoelectron spectroscopy and series impedance show that the catalyst is metallic property in virtue of exposed mental Ni in $Ni(OH)_2 \cdot NiO/FeOOH$(OCE). The volume ratio of hydrogen to oxygen (about 2:1) indicates overall water splitting by the double electrode system. When the volume ratio of hydrogen to oxygen is 2:1, the Faraday efficiency of H_2 or O_2 is close to 100%. $Ni(OH)_2 \cdot NiO/FeOOH$(OCE) exhibits good stability for one month. The research results provide a feasible approach for finding low cost metallized catalysts to replace noble metal as water oxidation catalysts and improving the efficiency of water splitting.

Keywords: oxidation-corrosion equilibrium, surface treatment, water oxidation, water splitting, oxygen evolution reaction, metallization

Introduction

As a clean energy, hydrogen energy is expected to be widely used.[1] The obtaining hydrogen by water splitting is considered to be environment-friendly and efficient. The process of water splitting includes hydrogen evolution reaction (HER)[2] and oxygen evolution reaction (OER)[3]. However, the overpotential will be observed when the large current passes through the electrodes, which leads to large bias voltage or wideband-gap photocatalyst to drive the process.[4] IrO_x [5]and RuO_x[6] catalysts are commonly used for OER in water splitting. However, the catalytic performance, long-term stability and cost of IrO_x and RuO_x catalysts cannot meet the industrialization. In the previous report, the oxides or hydroxyl oxides based Fe and Ni expressed good catalytic effect on OER. FeNiOOH nanosheets were grown on FeNi foam by in-situ chemical oxidation as a novel 3D electrode for OER.[7] Dual electrocatalyst thin films of FeOOH and NiOOH as photogenerated hole extractors were prepared for solar-driven water splitting. Recently, to improve the electrocatalytic activity of Ni foam (good electrical conductivity and three-dimensional structure), our group converted the Ni foam into a high activity NiOOH/FeOOH heterostructure as water oxidation catalyst by three step strategy (surface acid treatment and electroplating and electrooxidation).[8] The overpotential of NiOOH/FeOOH heterostructure for OER was 257 mV, which was better than that of IrO_2/Ni foam (280 mV).

An ideal electrocatalyst needs not only higher catalytic activity, but also smaller internal resistance (i.e. metallization) and larger specific surface area. However, the conductivity of NiFe oxides or hydroxyl oxides is lower than that of metal. To enhance conductivity, the thickness of the catalyst should be thin. Inspired by above state, in this study, we prepare $Ni(OH)_2 \cdot NiO/FeOOH$ by oxidation-corrosion equilibrium (OCE) in acid solution. For comparison, we also treat Ni foam with the same method in alkaline solution. $Ni(OH)_2 \cdot NiO/FeOOH$ prepared by OCE exhibits superior catalytic activity. The $Ni(OH)_2 \cdot NiO/FeOOH$(OCE) needs only 232 mV overpotential to reach a current density of 10 mA cm^{-2}, which is smaller than those (242, 254 mV) for references $Ni(OH)_2 \cdot NiO/FeOOH$ prepared in NaOH alkaline solution and IrO_2/Ni foam. The $Ni(OH)_2 \cdot NiO/FeOOH$ (OCE) has high small charge transfer resistance. The volume ratio of hydrogen to oxygen (about 2:1) in the double electrode system and the Faraday efficiency of H_2 or O_2 is also evaluated.

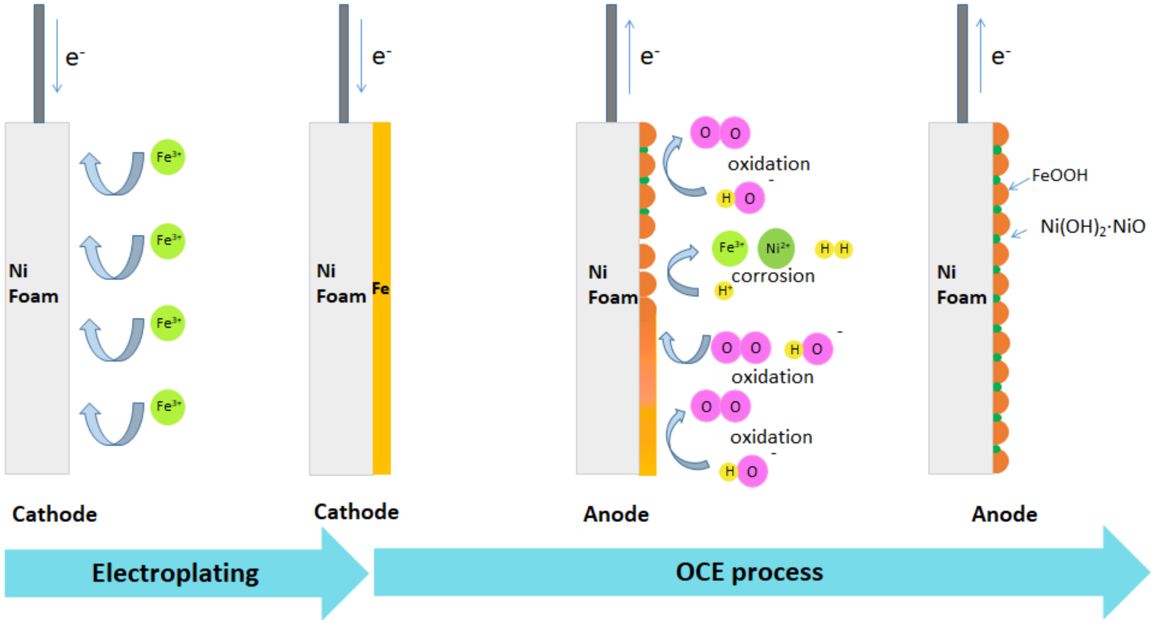

Figure 1. Schematic diagram of the process of $Ni(OH)_2{\cdot}NiO/FeOOH$ by oxidation-corrosion equilibrium (OCE) in 1M H_2SO_4 solution

Experimental Section

Preparation of $Ni(OH)_2{\cdot}NiO/FeOOH$ (OCE) and $Ni(OH)_2{\cdot}NiO/FeOOH$ (NaOH): first, Ni-foams (0.5 cm×1 cm) were treated in mixed acid (2 ml 65–68% HNO_3 solution and 6 ml 36–38% HCl solution). Then, the Ni-foams were soaked for 1 minutes and washed repeatedly with distilled water. Electroplating Fe on Ni-foam: Ni-foam treated by mixed acid was used as a cathode, Fe wire as an anode and 0.1 M $FeCl_3$ solution as an electrolyte for electroplating by potentiostat. The electroplating condition is as follows: the voltage is 3, 6, 9 V for 5 min, respectively. Fe-Ni foams were obtained. Electrooxidation: Fe-Ni foams were used as an anode and pure Ni-foam as a cathode. 1 M H_2SO_4 and 1 M NaOH solution were used as respective electrolyte for oxidation. The condition of oxidation treatment is that the constant current density of the potentiostat is 100 mA cm^{-2} and the oxidation time is 1 min. Finally, $Ni(OH)_2{\cdot}NiO/FeOOH$ (OCE) and $Ni(OH)_2{\cdot}NiO/FeOOH$ (NaOH) were obtained.

Preparation of IrO_2/Ni-Foam by hydrothermal synthesis: $IrCl_3$, 0.9632 g, was solved in 10 ml H_2O. Poly(ethylene glycol) (MV: 6000), 1.0 g, was dissolved in 10 ml H_2O and 0.6 g NaOH was dissolved in 10 ml H_2O. The above three solutions were mixed and transferred to a Teflon-lined autoclave. The Ni-foam was immersed in Teflon-lined autoclave containing the mixed solution.

The Teflon-lined autoclave was heated at 200 ℃ for 15 h. Preparation of Pt/Ni-Foam by chemical reduction is referenced to our previous report.[8]

Characterization:

The morphology characteristics of the sample was done using SEM (Thermo Fisher Scientific FIB-SEM GX_4). The X-ray photoelectron spectroscopy (XPS) was carried out in a Thermo ESCALAB 250. For three-electrode catalytic activity characterization, linear sweep voltammetry (LSV) test was performed on CHI760E electrochemical workstation: $Ni(OH)_2{\cdot}NiO/FeOOH$ (OCE), $Ni(OH)_2{\cdot}NiO/FeOOH$ (NaOH) and IrO_2/Ni-foam were used as working electrodes respectively, Ag/AgCl (1 M KCl) as the reference electrode, Ni-foam as the auxiliary electrode, and 1.0 M KOH solution as the electrolyte; voltage range 2–0 V for OER; scanning speed 0.001 V s^{-1} with the scan direction from positive to negative. For dual-electrode LSV test, $Ni(OH)_2{\cdot}NiO/FeOOH$ (OCE), $Ni(OH)_2{\cdot}NiO/FeOOH$ (NaOH) and IrO_2/Ni-foam were used as anode respectively, Ni-foam as cathode, and 1.0 M KOH solution as electrolyte. Test conditions were as follows: voltage range of 2–0 V and scanning speed of 0.001 V s^{-1} with the scan direction from positive to negative.

For three-electrode CV test, $Ni(OH)_2{\cdot}NiO/FeOOH$ (OCE), $Ni(OH)_2{\cdot}NiO/FeOOH$ (NaOH), IrO_2/Ni-foam, Ni-foam were used as working electrodes respectively, Ag/AgCl (1 M KCl) as the reference electrode, Ni-foam as the auxiliary electrode, and 1.0 M KOH solution as the electrolyte. Test conditions were as follows: voltage range of 0–0.1 V and scanning speed of 1, 5, 10 ,30 ,50 and 70 mV s^{-1}, with the scan direction from negative to positive. H_2 /O_2 collection and measurement: the hydrogen and oxygen in the two-electrode system were collected and measured by potentiometer at the current density of 13 mA cm^{-2}. H-type electrolyzer is connected to the collection device. The anode is $Ni(OH)_2{\cdot}NiO/FeOOH$ (OCE) and the cathode is Pt/Ni foam. When the volume of O_2 was 0.5, 1, 1.5, 2, 2.5 and 3 mL, we recorded the volume of H_2.

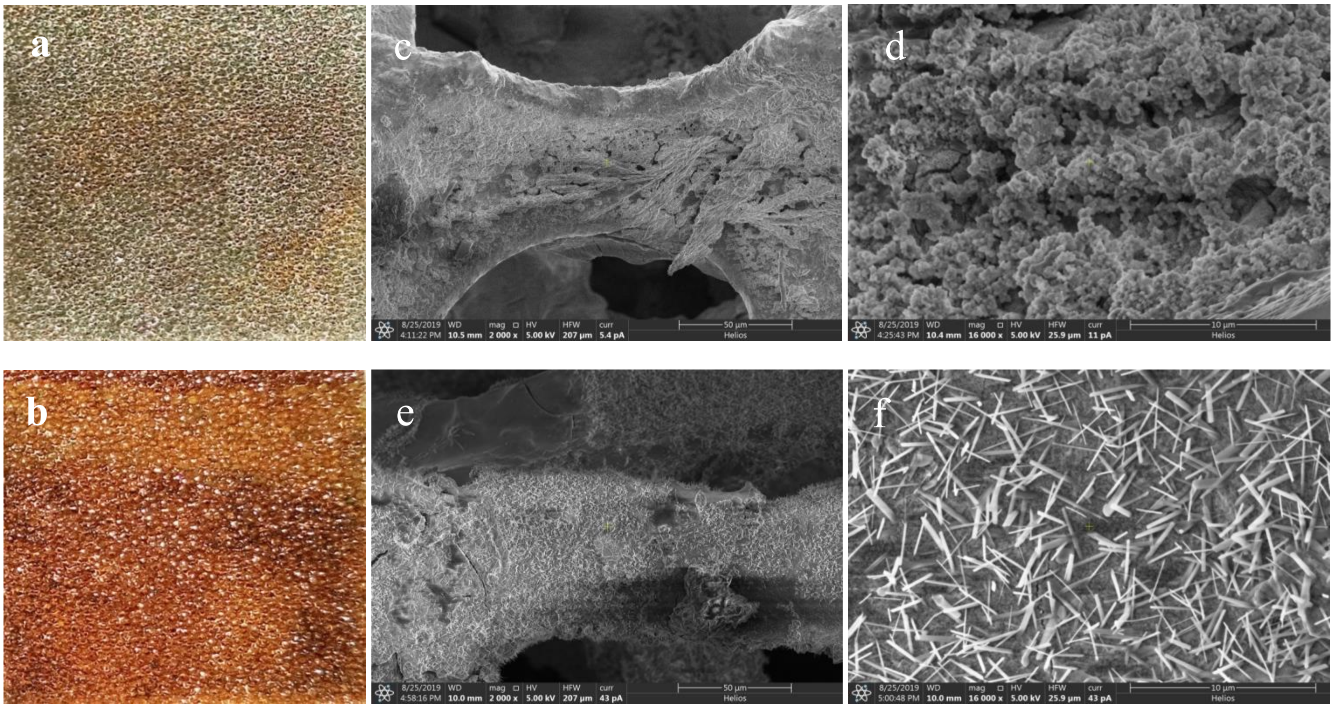

Figure 2 (a) Photo of $Ni(OH)_2{\cdot}NiO/FeOOH$(OCE) on Ni foam electrode. (b) photo of $Ni(OH)_2{\cdot}NiO/FeOOH$ (NaOH) on Ni foam electrode. (c, d) the morphology of $Ni(OH)_2{\cdot}NiO/FeOOH$(OCE). (e, f) the morphology of $Ni(OH)_2{\cdot}NiO/FeOOH$ (NaOH).

Results and Discussion

Schematic diagram of OCE method for $Ni(OH)_2{\cdot}NiO/FeOOH$ is shown in Figure 1. The detailed preparation process is described in the experimental section. Firstly, Fe-Ni foam as anode was prepared by electroplating a layer of iron on Ni foam as shown in Figure 1, and then immersed in 1M H_2SO_4 acid solution for OCE. The process of OCE is as follows: Driven by positive potential, OH^- anions in 1M H_2SO_4 solution accumulate around the anode and lose electrons to produce O_2. Fe on the surface of Fe-Ni foam combines with H^+, OH^- and O_2 to form FeOOH. Meanwhile, as an inverse process of OCE, H_2SO_4 solution corrode (dissolve) FeOOH oxide layer. In addition, $Ni(OH)_2$ on Ni foam is also formed by OCE. When the oxidation rate is equal to the corrosion rate, $Ni(OH)_2{\cdot}NiO/FeOOH$ on Ni foam is formed and arrives steady-state. The chemical reaction equations (1-7) for the whole process are listed as follows. As reference, Fe-Ni foam treated in 1 M NaOH basic solution were also prepared by with the same step as anode in 1 M H_2SO_4 acid solution.

$OH^- - e^- \rightarrow H_2O + O_2\uparrow$ (1)
$Fe + H^+ \rightarrow Fe^{2+} + H_2\uparrow$ (2)
$OH^- + O_2 + Fe^{2+} \rightarrow FeOOH$ (3)
$FeOOH + H^+ \rightarrow Fe^{3+} + H_2O + OH^-$ (4)
$Ni + H^+ \rightarrow Ni^{2+} + H_2\uparrow$ (5)
$OH^- + Ni^{2+} \rightarrow Ni(OH)_2$ (6)
$Ni(OH)_2 + H^+ + O_2 \rightarrow NiO + H_2O$ (7)

The photos of $Ni(OH)_2{\cdot}NiO/FeOOH$ (OCE) and $Ni(OH)_2{\cdot}NiO/FeOOH$ (NaOH) are shown in the Figure 2a, 2b, respectively. The results show that the surface of $Ni(OH)_2{\cdot}NiO/FeOOH$ (OCE) is green, while the surface of $Ni(OH)_2{\cdot}NiO/FeOOH$ (NaOH) is brownish red. The morphology of $Ni(OH)_2{\cdot}NiO/FeOOH$ (OCE) were characterized by scanning electron microscopy (SEM), as shown in Figure 2c, 2d. Rough surface of $Ni(OH)_2{\cdot}NiO/FeOOH$ (OCE) is observed in Figure 2d. As a contrast, the morphology of $Ni(OH)_2{\cdot}NiO/FeOOH$ (NaOH) is shown in Figure 2e, 2f. A large number of nanorods are attached to the surface of Ni-foam as shown in Figure 2f. The surface chemistry information of $Ni(OH)_2{\cdot}NiO/FeOOH$ (OCE) was characterized using X-ray photoelectron spectroscopy (XPS). To determine the ascription of each peak, "XPS Peak" software were used to fit XPS curves. All fitting data are shown in the Table S1-S4. (reference supporting information). Six different peaks are observed in the Ni 2p XPS curve of $Ni(OH)_2{\cdot}NiO/FeOOH$ (OCE) as shown in Figure 3a, which indicate coexistence of different chemical valences for Ni species. The peak area at 861.48 eV and at 873.83 eV are originated from NiO, which indicates that they are the main forms on the surface. Compared with $Ni(OH)_2{\cdot}NiO/FeOOH$ (NaOH) (Figure 3b), the XPS spectrum of $Ni(OH)_2{\cdot}NiO/FeOOH$ (OCE) shows an additional peak at 852.22 eV corresponding to mental Ni, which indicates that $Ni(OH)_2{\cdot}NiO/FeOOH$ (OCE) has metallic property, that is, it has good conductivity. While the peak area of Ni $(OH)_2$ at 855.50 eV for $Ni(OH)_2{\cdot}NiO/FeOOH$ (NaOH) is dominant, which indicates that $Ni(OH)_2$ is the main existing form on the surface of $Ni(OH)_2{\cdot}NiO/FeOOH$ (NaOH). Surface chemical states of Fe species on $Ni(OH)_2{\cdot}NiO/FeOOH$ (OCE) were also analyzed by XPS. Two different peaks at 712.20 eV，724.36eV are observed in the Fe 2p XPS curve of $Ni(OH)_2{\cdot}NiO/FeOOH$ (OCE) (Figure 3c). The Fe 2p XPS spectra displays a pair of spin-orbit doublets. The results indicate that Fe on the surface of $Ni(OH)_2{\cdot}NiO/FeOOH$ (OCE) is mostly FeOOH. By contrast, the ratio of 2p 3/2FeOOH to 2p 1/2 FeOOH on the surface of $Ni(OH)_2{\cdot}NiO/FeOOH$ (OCE) is higher than that of $Ni(OH)_2{\cdot}NiO/FeOOH$ (NaOH) in Figure 3d.

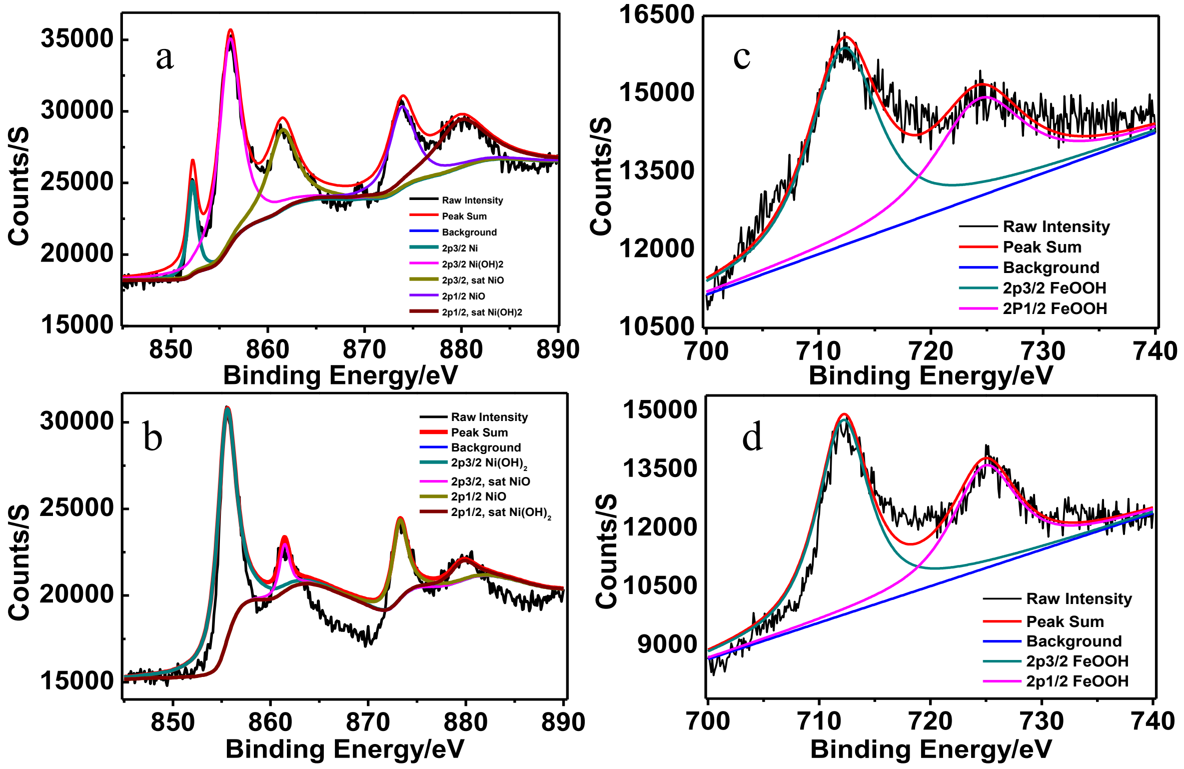

Figure 3 (a) Ni 2p XPS curve of $Ni(OH)_2 \cdot NiO/FeOOH$ (OCE); (b) Ni 2p XPS curve of $Ni(OH)_2 \cdot NiO/FeOOH$ (NaOH); (c)Fe 2p XPS curve of $Ni(OH)_2 \cdot NiO/FeOOH$ (OCE); (d) Fe 2p XPS curve of $Ni(OH)_2 \cdot NiO/FeOOH$ (NaOH).

The electrochemical performance of $Ni(OH)_2 \cdot NiO/FeOOH$ (OCE) as an OER electrocatalyst was evaluated in three and two electrode configuration using 1.0 M KOH as the electrolyte. $Ni(OH)_2 \cdot NiO/FeOOH$(NaOH), IrO_2/Ni foam and Ni foam were also researched as reference group. OER characteristics of linear sweep voltammetry (LSV) based different electrodes are shown in Figure 4 at a scan rate of 1 mV s^{-1}, with the scan direction from positive to negative on the reversible hydrogen electrode (RHE) scale. The specific data are shown in the Table 1. $Ni(OH)_2 \cdot NiO/FeOOH$(OCE) shows superior OER activity to $Ni(OH)_2 \cdot NiO/FeOOH$(NaOH), IrO_2/Ni foam and Ni foam. The overpotential at a current density of 10 mA cm^{-2} is a significant performance parameter. In a three-electrode configuration (Figure 4a), $Ni(OH)_2 \cdot NiO/FeOOH$(OCE) electrode requires η_{OER} of 232 mV to reach a (projected geometric area) current density of 10 mA cm^{-2}, which is 10, 22 and 196 mV less than those of $Ni(OH)_2 \cdot NiO/FeOOH$(NaOH), IrO_2/Ni foam and Ni foam, respectively. In addition, the value of OER onset potential of $Ni(OH)_2 \cdot NiO/FeOOH$(OCE), $Ni(OH)_2 \cdot NiO/FeOOH$ (NaOH), IrO_2/Ni foam and Ni foam are 1.46, 1.47, 1.50 and 1.72 V, respectively. To study the OER kinetics of catalysts, we fitted LSV curve of $Ni(OH)_2 \cdot NiO/FeOOH$(OCE), $Ni(OH)_2 \cdot NiO/FeOOH$(NaOH), IrO_2/Ni foam and Ni foam according to Tafel equation to obtain the corresponding Tafel slope (Figure 4b). The lower Tafel slope of electrode means more efficient electron transfer and faster reaction rate. Compared with other samples, the lower Tafel slope (86.6 mV dec^{-1}) of $Ni(OH)_2 \cdot NiO/FeOOH$(OCE) demonstrates the significant improvement in the OER kinetics. We further characterized performance of $Ni(OH)_2 \cdot NiO/FeOOH$(OCE) in the two-electrode configuration (Pt/Ni foam as cathode) as shown in the Figure 4c. $Ni(OH)_2 \cdot NiO/FeOOH$(OCE) electrode requires η_{OER} of 454 mV to reach a current density of 10 mA cm^{-2}, which is 42, 51 and 191 mV less than those of $Ni(OH)_2 \cdot NiO/FeOOH$ (NaOH), IrO_2/Ni foam and Ni foam, respectively. It is worth mentioning that both η_{OER} and OER onset potential required by $Ni(OH)_2 \cdot NiO/FeOOH$(OCE) are superior to $Ni(OH)_2 \cdot NiO/FeOOH$ (NaOH).

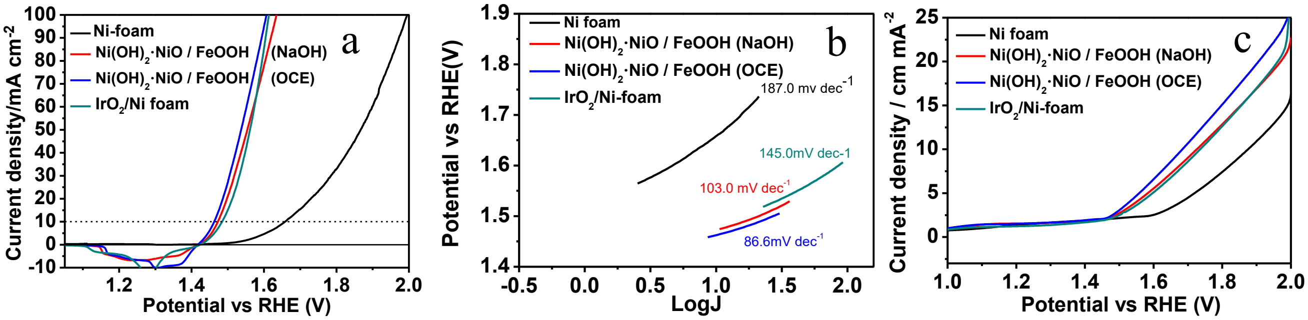

Figure 4 Electrochemical performance of pure Ni foam, $Ni(OH)_2 \cdot NiO/FeOOH$(NaOH), $Ni(OH)_2 \cdot NiO/FeOOH$(OCE) and IrO_2/Ni foam by linear sweep voltammetry in 1 M KOH aqueous electrolyte. (a) OER characteristics of different electrodes in a three-electrode, scanned in the direction from positive to negative potential on the RHE scale. (b)Tafel plots of different electrodes. (c) OER characteristics of different electrodes in the two-electrode configuration, when Pt/Ni-foam were used as hydrogen evolution electrodes. All scan rates were 1 mV s^{-1}.

Table 1. The overpotential of different electrode materials for OER to reach a current density of 10 mA cm^{-2} (Pt/Ni foam is hydrogen evolution electrode)

	Ni-foam	$Ni(OH)_2 \cdot NiO/FeOOH$ (NaOH)	$Ni(OH)_2 \cdot NiO$ / FeOOH (OCE)	IrO_2/Ni foam
three-electrode configuration	428	242	232	254
two-electrode configuration	——	496	454	505

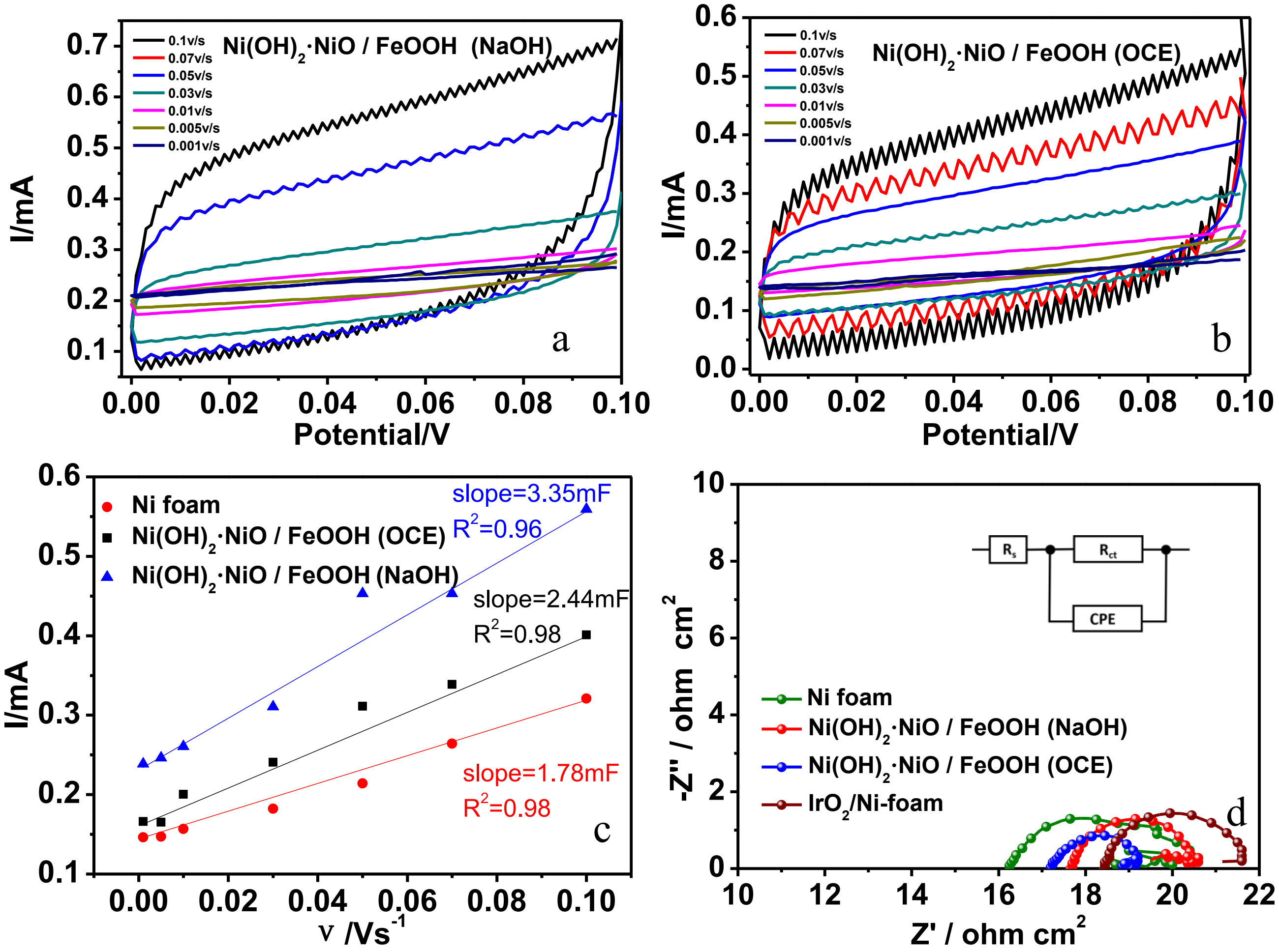

Figure 5 (a,b) Cyclic voltammograms for $Ni(OH)_2 \cdot NiO/FeOOH$(NaOH), $Ni(OH)_2 \cdot NiO/FeOOH$(OCE), respectively. (c) The capacitive currents with a scan rate of 1, 5, 10, 30, 50, 70, and 100mV s^{-1} in 1 M KOH. (d) Nyquist plots of in two-electrode electrolyzers (anode: $Ni(OH)_2 \cdot NiO/FeOOH$(OCE), $Ni(OH)_2 \cdot NiO/FeOOH$(NaOH) and IrO_2/Ni-foam; cathode: pure Ni-foam) recorded at an applied potential of 2.1 V with a frequency range of 1 MHz to 0.05 Hz in 1 M KOH.

Table 2 The fitting data of R_s and R_{ct} values of Pure Ni-foam, $Ni(OH)_2{\cdot}NiO/FeOOH(NaOH)$, $Ni(OH)_2{\cdot}NiO/FeOOH(OCE)$, and IrO_2/Ni-foam.

	R_s / Ω cm ²	R_{ct} / Ω cm ²
Pure Ni-foam	16.13	4.48
$Ni(OH)_2{\cdot}NiO/FeOOH(NaOH)$	17.68	2.85
$Ni(OH)_2{\cdot}NiO/FeOOH(OCE)$	17.24	2.04
IrO_2/Ni-foam	18.45	3.06

To verify the relationship between the intrinsic activity and the surface structure of $Ni(OH)_2{\cdot}NiO/FeOOH(OCE)$, the electrochemically active surface area (EASA) was evaluated by cyclic voltammetry (CV). The EASA is estimated by determining the double-layer capacitance from CV according to the previous reports.[8] More specifically, it is obtained by the electrochemical double-layer capacitance of the catalytic surface, which is in accordance with formula EASA = C_{DL}/C_S, where C_S is the specific capacitance of the sample or the capacitance of an atomically smooth planar surface of the material per unit area under identical electrolyte conditions. The general specific capacitance used in our experiments is C_S = 0.040 mF cm^{-2} in 1 M KOH. According to formula $i_c = \nu C_{DL}$, the potential is scanned in a nonfaradaic potential window (here is 0 to 0.1 V vs. RHE) at varying scan rates (Figure 5a,b). The obtained current at 0.05 V (vs. RHE) plotted against the scan rate gives a straight line (Figure 5c), in which the slopes give corresponding C_{DL} values. Impressively, the C_{DL} of $Ni(OH)_2{\cdot}NiO/FeOOH(OCE)$ is calculated to be 2.44 mF, which is lower than that (3.35 mF) of $Ni(OH)_2{\cdot}NiO/FeOOH(NaOH)$. The values of EASA for $Ni(OH)_2{\cdot}NiO/FeOOH(OCE)$ and $Ni(OH)_2{\cdot}NiO/FeOOH$ (NaOH) are 61.00 and 83.75 cm^{-2}, respectively. Although the surface area of $Ni(OH)_2{\cdot}NiO/FeOOH(OCE)$ is smaller than $Ni(OH)_2{\cdot}NiO/FeOOH(NaOH)$, $Ni(OH)_2{\cdot}NiO/FeOOH(OCE)$ has higher activity on a single active site. The roughness factor (RF) was also calculated by taking the estimated EASA and dividing it by the geometric area of the electrode 0.5 cm^{-2}. The RF of $Ni(OH)_2{\cdot}NiO/FeOOH(OCE)$ and $Ni(OH)_2{\cdot}NiO/FeOOH(NaOH)$ are 122.0 and 167.5, respectively.

To investigate the charge transfer between solid-liquid interface, charge transfer resistance (R_{ct}) and series resistance (R_s) of $Ni(OH)_2{\cdot}NiO/FeOOH(OCE)$, $Ni(OH)_2{\cdot}NiO/FeOOH(NaOH)$, IrO_2/Ni foam and Ni foam were evaluated by electrochemical impedance spectroscopy (EIS) as shown in the Figure 5d. In the circuit diagram, R_s comes from the resistance of two-electrode electrolyzers (electrode wire, electrode and electrolyte). R_{ct} results from the resistance of charge transfer between catalyst and water splitting reaction. The semi-circular diameter reflects the R_{ct}. We used Z-view software to fit the data to get R_s and R_{ct} values. The specific data are shown in Table 2. The R_s values of $Ni(OH)_2{\cdot}NiO/FeOOH(OCE)$, $Ni(OH)_2{\cdot}NiO/FeOOH$ (NaOH) and IrO_2/Ni foam are 17.24, 17.68 and 18.45 Ω cm², respectively. Obviously, the R_s value of $Ni(OH)_2{\cdot}NiO/FeOOH(OCE)$ is the smallest, which indicates that the electrode is more metallic. Impressively, compared with $Ni(OH)_2{\cdot}NiO/FeOOH(NaOH)$ and IrO_2/Ni foam(3.06Ω), $Ni(OH)_2{\cdot}NiO/FeOOH(OCE)$ possesses smaller R_{ct}. The results demonstrated that $Ni(OH)_2{\cdot}NiO/FeOOH$ formed by OCE method can guarantee rapid electron transfer to promote the OER activity.

The practical faraday efficiency and stability performance of $Ni(OH)_2{\cdot}NiO/FeOOH(OCE)$ were carried out. The devices to collect gas (hydrogen and oxygen) and measure gas constants were built, as previous report.[8] The volume ratio of hydrogen to oxygen produced in the device is about 2:1 as shown in Figure 6a， which indicates the double-electrode system ($Ni(OH)_2{\cdot}NiO/FeOOH$ (OCE) as anode, pure Ni foam as cathode) presents almost overall water splitting. In addition, Faraday efficiency is the conversion efficiency of electric energy into special chemical energy (H_2 or O_2). The formula is Faraday efficiency =m*n*F/(I*t), where m is moles of the product, n is the number of reaction transfer electrons, F is the Faraday constant, I is the current and t is the time. The Faraday efficiency of hydrogen or oxygen is close to 100% when the volume ratio of hydrogen to oxygen is about 2:1(Figure 6a). The results show that almost the electric energy has been converted into chemical energy (obtained H_2 or O_2) by water electrolysis. Finally, the stability of $Ni(OH)_2{\cdot}NiO/FeOOH(OCE)$ in the two-electrode system (the Pt/Ni foam as cathode and $Ni(OH)_2{\cdot}NiO/FeOOH(OCE)$ as anode) was studied as shown in Figure 6b. The continuous potential shows almost no change during one month, which suggests the high durability of $Ni(OH)_2{\cdot}NiO/FeOOH(OCE)$ in a long-term OER under 1 M KOH alkaline conditions.

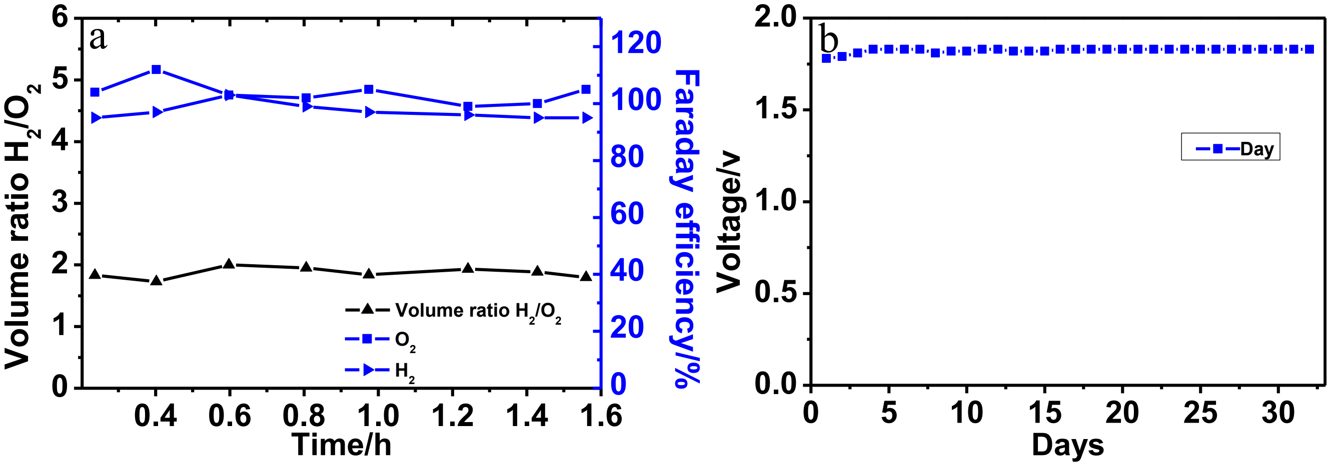

Figure 6. (a) Hydrogen oxygen ratio and Faraday efficiency of $Ni(OH)_2{\cdot}NiO/FeOOH$ (OCE) as anode, respectively. (b) The stability of double-electrode system driven by constant current density of 9.3 mA cm^{-2} (anode: $Ni(OH)_2{\cdot}NiO/FeOOH$ (OCE); cathode: Pt/Ni foam)

Conclusion

In conclusion, in this study, we prepared $Ni(OH)_2{\cdot}NiO/FeOOH$ by oxidation-corrosion equilibrium method (OCE) in acid solution for as water oxidation catalyst. As reference, $Ni(OH)_2{\cdot}NiO/FeOOH$(NaOH) were prepared in alkaline solution with the same method. $Ni(OH)_2{\cdot}NiO/FeOOH$ prepared by OCE exhibits superior catalytic activity as water oxidation catalyst to $Ni(OH)_2{\cdot}NiO/FeOOH$(NaOH). $Ni(OH)_2{\cdot}NiO/FeOOH$(OCE) needs only 232 mV to reach a current density of 10 mA cm^{-2}, while it is 254 mV for traditional IrO_2/Ni foam. The metallic $Ni(OH)_2{\cdot}NiO/FeOOH$(OCE) is favorable for the rapid interface electron exchange between Ni $(OH)_2/FeOOH$(OCE) and water oxidation reaction. $Ni(OH)_2/FeOOH$(OCE) exhibit overall water splitting, excellent Faraday efficiency and good stability.

ASSOCIATED CONTENT

Supporting Information

This material is available free of charge via the Internet at http://pubs.acs.org.

Tables: Fitting parameter in XPS curve of Ni 2p chemical distribution on $Ni(OH)_2{\cdot}NiO/FeOOH$(OCE); Fitting parameter in XPS curve of Fe 2p chemical distribution on $Ni(OH)_2{\cdot}NiO/FeOOH$(OCE); Fitting parameter in XPS curve of Ni 2p chemical distribution on $Ni(OH)_2{\cdot}NiO/FeOOH$(NaOH); Fitting parameter in XPS curve of Fe 2p chemical distribution on $Ni(OH)_2{\cdot}NiO/FeOOH$(NaOH).

AUTHOR INFORMATION

Corresponding Author

*E-mail: zhouhuaweiopv@163.com

*E-mail: yinjieily@163.com

ACKNOWLEDGMENT

This work was financially supported by the Shandong Province Natural Science Foundation (Grant No. ZR2019MB021).

REFERENCES

1. Schlapbach, L.; Zuttel, A., Hydrogen-storage materials for mobile applications. *Nature* **2001,** *414* (6861), 353-358.

2. Zou, X. X.; Zhang, Y., Noble metal-free hydrogen evolution catalysts for water splitting. *Chemical Society Reviews* **2015,** *44* (15), 5148-5180.

3. Liang, Y. Y.; Li, Y. G.; Wang, H. L.; Zhou, J. G.; Wang, J.; Regier, T.; Dai, H. J., Co3O4 nanocrystals on graphene as a synergistic catalyst for oxygen reduction reaction. *Nature Materials* **2011,** *10* (10), 780-786.

4. Masa, J.; Barwe, S.; Andronescu, C.; Sinev, I.; Ruff, A.; Jayaramulu, K.; Elumeeva, K.; Konkena, B.; Roldan Cuenya, B.; Schuhmann, W., Low Overpotential Water Splitting Using Cobalt-Cobalt Phosphide Nanoparticles Supported on Nickel Foam. *Acs Energy Letters* **2016,** *1* (6), 1192-1198.

5. Li, L.; Wang, B.; Zhang, G. W.; Yang, G.; Yang, T.; Yang, S.; Yang, S. C., Electrochemically Modifying the Electronic Structure of IrO(2)Nanoparticles for Overall Electrochemical Water Splitting with Extensive Adaptability. *Advanced Energy Materials* **2020,** *10* (30): 2001600.

6. Zhang, G. W.; Wang, B.; Li, L.; Yang, S.; Liu, J. M.; Yang, S. C., Tailoring the electronic structure by constructing the heterointerface of RuO2-NiO for overall water splitting

with ultralow overpotential and extra-long lifetime. *Journal of Materials Chemistry A* **2020,** *8* (36), 18945-18954.

7. Wang, Z.; Lei, Q.; Wang, Z.; Yuan, H.; Cao, L.; Qin, N.; Lu, Z.; Xiao, J.; Liu, J., In-situ synthesis of free-standing FeNi-oxyhydroxide nanosheets as a highly efficient electrocatalyst for water oxidation. *Chemical Engineering Journal* **2020,** *395:* 125180.

8. Yin, J.; Di, F. F.; Guo, J. X.; Zhang, K. X.; Xu, W. L.; Wang, Y. Y.; Shi, S. Z.; Chai, N.; Chu, C. F.; Wei, J. Z.; Li, W. Z.; Shao, X.; Pu, X. P.; Zhang, D. F.; Ren, X. Z.; Wang, J.; Zhao, J. S.; Zhang, X. X.; Wei, X. T.; Wang, F.; Zhou, H. W., Tuning Ni-Foam into NiOOH/FeOOH Heterostructures toward Superior Water Oxidation Catalyst via Three-Step Strategy. *Acs Omega* **2018,** *3* (9), 11009-11017.

Table of Contents